HortScience 60(8):1268–1275. 2025. https://doi.org/10.21273/HORTSCI18602-25

Development of a Callus Culture for Increased Yield of Secondary Metabolite Production in Spider Lily (*Crinum asiaticum* L.)

Yashika Bansal, A Mujib, Jyoti Mamgain, Mohammad Mohsin, and Afeefa Nafees
Cellular Differentiation and Molecular Genetics Section, Department of Botany, Jamia Hamdard, New Delhi 110062, India

Yaser Hassan Dewir
Department of Plant Production, College of Food and Agricultural Sciences, King Saud University, P.O. Box 2460 Riyadh 11451, Saudi Arabia

Katalin Magyar-Tábori
Research Institute of Nyíregyháza, Institutes for Agricultural Research and Educational Farm, University of Debrecen, P.O. Box 12, 4400 Nyíregyháza, Hungary

Keywords. 2, 2-diphenyl-1-picrylhydrazyl, callus, in vitro propagation, peroxidase, phytocompounds, superoxide dismutase

Abstract. ***Crinum asiaticum*** **is an important medicinal and ornamental plant known for its anticancer, analgesic, antiviral, anti-inflammatory, and antifungal properties attributable to its diverse classes of compounds. However, the plant is being overexploited in its native habitat because of its therapeutically significant phytocompounds, leading to a decline in its population. Thus, this study aimed to establish a callus culture system and detect and compare the metabolites content in both in vivo and in vitro regenerated calli. In vitro callus culture of *C. asiaticum* was initiated from bulb scales on Murashige and Skoog medium supplemented with different concentrations of plant growth regulators. Afterward, gas chromatography-mass spectrometry (GC-MS) analyses of methanol extracts of bulb scale and bulb scale-derived calli were performed. The antioxidant potentials of both the samples were evaluated by determining the 2, 2-diphenyl-1-picrylhydrazyl (DPPH), peroxidase (POD), and superoxide dismutase (SOD) activities. The medium fortified with 0.5 mg/L 2,4-dichlorophenoxyacetic acid (2, 4-D) produced profuse callus with a frequency of 95.83%. The GC-MS analysis of both extracts confirmed the presence of 34 and 31 bioactive compounds, respectively. Various phytochemicals such as gamma-sitosterol, squalene, vitamin E, linolenic acid, and guanosine were present in both extracts. The results of all the antioxidant assays (DPPH, POD, and SOD) revealed higher antioxidant activities in callus compared with those in bulb scale tissue. This study proved the potential of using callus culture on a larger scale as a source of several important secondary metabolites in the pharmaceutical industry.**

Medicinal plants serve as a vital source for the development of health-promoting biomaterials because of their diverse bioactive compounds with therapeutic potential (Luo et al. 2024). Modern advancements in natural biomaterials have significantly enhanced health applications, for instance, the development of surface-functionalized blood-contacting biomaterials has shown great promise in preventing coagulation and promoting hemostasis (Wang et al. 2023). The species *Crinum asiaticum*, an Amaryllidaceae family member, is a perennial bulbous herbaceous plant that grows up to 2 m tall and has green leaves. It grows well in subtropical and tropical regions with fertile and moist soil and requires light shade to full sun (Mahomoodally et al. 2021). It is an important medicinal and ornamental plant that is abundantly found in mainland Japan, China, India, Sri Lanka, Myanmar, Thailand, and Malaysia (Rahman et al. 2012). In Ayurveda, it is referred to as naagadamani; however, in Malaysian and Papua New Guinean dialects, it is called Bakong, spider lily, *Crinum* lily, and poison bulb in English (Sura and Solleti 2020). In traditional medicine systems it has been used to treat earaches, vomiting, contusions, fractures, inflammatory joints, and sprains. Additionally, the plant has other important therapeutic effects, including anticancer, analgesic, antiviral, antimalarial, antibacterial, antifungal, and anti-inflammatory properties (Rakhi et al. 2024; Tan et al. 2019). Furthermore, this plant contains the following important phytoconstituents: Norgalanthamine, crinamine, flexinine, pratorimine, hamayne, stigmasterol, cycloartenol, cycloaudenol, ambeline, hippadine, ungeremine, criasbetaine, criasidine, and lycorine and its glucoside (Danquah et al. 2022). Globally, galanthamine (an isoquinoline alkaloid) is recommended as a medication for patients with dementia, schizophrenia, and Alzheimer's diseases because it enhances cholinergic nicotinic neurotransmission in central and peripheral nervous systems by selectively inhibiting acetylcholine esterase (Priyadharshini et al. 2020; Syeed et al. 2024). Lycorine exhibits anticancerous and cytotoxic activities (Georgiev et al. 2020). Flexinine possesses antiviral and cytotoxic properties (Ka et al. 2021). Stigmasterol possesses antiosteoarthritis, anti-inflammatory, immunomodulatory, antiparasitic, and neuroprotective properties (Bakrim et al. 2022; Bansal et al. 2023).

Generally, propagation of *C. asiaticum* is achieved by means of seeds and bulbs. However, as a result of excessive utilization of valuable phytocompounds, poor seed germination, and poor viability rates, this plant is threatened in their natural habitats (Sanyal et al. 2023). Modern biotechnological techniques have superseded traditional breeding approaches for multiple plants because of the presence of several phytocompounds (Bansal et al. 2024a). Additionally, micropropagation is an alternative effective technique for quick multiplication and proliferation of plants, production of pathogen free stocks, genetically modifying clones, and obtaining therapeutically important bioactive substances within a shorter period of time without the use of field farming (Murthy et al. 2023). Among other techniques, callogenesis has emerged as a valuable tool to produce plant-derived medicinal compounds (PDMCs) at a commercial scale (Cardoso et al. 2019) because almost every plant portion has the capability to generate callus and can be monitored indefinitely with regular subculturing (Efferth 2019). The callus culture often exhibits a wide range of secondary metabolites that are not limited to any particular group of compounds (Benjamin et al. 2019).

Gas chromatography-mass spectrometry (GC-MS) techniques allow detection and validation of different phytocompounds such as alkaloids, phenols, saponins, tannins, alcohol, steroids, and glycosides based on their respective retention times and spectra (Ashwini and Rajanna 2022). Several investigations demonstrated the importance of a number of variables and their influences on in vitro development of callus cultures, such as the plant genotype, explant type, plant growth regulators (PGRs), and media composition of media (Fatima et al. 2024; Hazrati et al. 2022). Such factors usually cause an increase in reactive oxygen species (ROS) such as superoxide, hydrogen peroxide, and hydroxyl radical, which inhibit cell growth and differentiation, resulting in oxidative damage and subsequent cell death (Bibi et al. 2018; Ozden and Karaaslan 2011). To cope with harmful effects of such radicals, plants have inbuilt antioxidative defense systems such as the presence of antioxidant enzymes, including superoxide dismutase (SOD), catalase (CAT), and peroxidase (POD) to prevent cellular damages. Recent innovations in the extraction of secondary metabolites from medicinal plants have integrated advanced computational techniques to

enhance efficiency. Wan et al. (2024) used an ant colony algorithm-enabled back propagation neural network combined with response surface methodology to optimize the ultrasonic extraction of alkaloids from safflower seeds, thus achieving improved antioxidant activity. The present investigation aimed to optimize a callus induction protocol from bulb scales of *C. asiaticum*. This study is first of its kind to identify the metabolites present tissues raised in vivo and in vitro using GC-MS techniques. Nonenzymatic antioxidant [2, 2-diphenyl-1-picrylhydrazyl (DPPH)] and antioxidant enzymatic assays (SOD and POD) were conducted to evaluate the antioxidative capacity of *C. asiaticum* tissues.

Materials and Methods

Chemicals and reagents

All of the solvents and chemicals used during this investigation were of analytical grade and purchased from Himedia (Mumbai, India), SRL (Mumbai, India), and Sigma-Aldrich (St. Louis, MO, USA). The chemicals and reagents included Murashige and Skoog (MS) medium (Murashige and Skoog 1962), PGRs, methanol (high-performance liquid chromatography grade), DPPH, guaiacol, hydrogen peroxide, ethylenediaminetetraacetic acid (EDTA), polyvinylpyrrolidone (PVP), Triton X-100, Nitro blue tetrazolium (NBT), riboflavin, methionine, and sodium carbonate.

Plant material, sterilization, and culture conditions

In this study, healthy bulbs of *C. asiaticum* were collected from Herbal Garden, Jamia Hamdard, New Delhi, India, and they were identified by Dr. S. N. Khan (Taxonomist, Jamia Hamdard, India) (voucher specimen number: JH/BOT/DAC/2022/07). The inner scales of the bulbs were used as explants. The surface sterilization for callus induction of the *Crinum* bulb scales was performed according to the protocol reported by Bibi et al. (2018). First, the explants were washed under running tap water, rinsed with 70% (v/v) ethanol for 2 min, and then rinsed with distilled water thrice. Finally, the explants were treated with 0.1% (w/v) mercuric chloride solution for 2 min and then rinsed with distilled water thrice. The surface-sterilized explants were then cut into small segments (4–5 cm) and placed into glass test tubes (16 × 125 mm in size) containing 0.8% (w/v) agar-solidified MS medium with 3% (w/v) sucrose and various concentrations of PGRs with a pH adjusted to 5.8. Afterward, the cultures were kept in a growth chamber with an air temperature of 24 °C (±2 °C), 16-h photoperiod, and 30 $\mu mol \cdot m^{-2} \cdot s^{-1}$ radiation provided by cool white fluorescent light at a relative humidity of 50% to 55%.

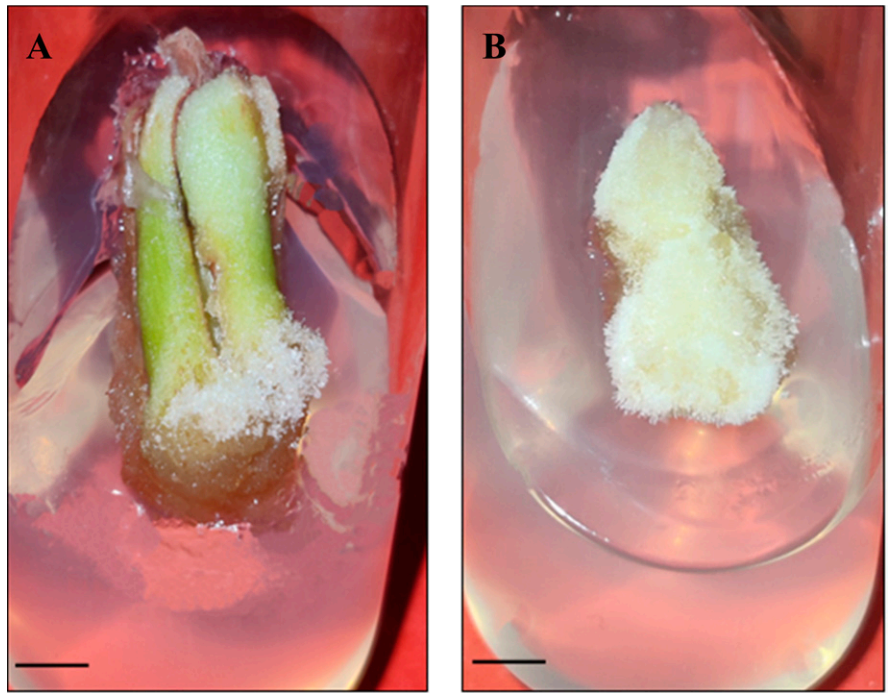

Fig. 1. Callus induction and growth from bulb scale explants of *C. asiaticum*. (**A**) Callus initiation after 1 week of inoculation. (**B**) Callus proliferation after 3 weeks. (Bars = 0.5 cm.)

Callus induction and proliferation

Sterilized inner scales of bulbs were inoculated on MS supplemented with varying concentrations (0.25–1.0 mg/L) of auxins [2,4-dichlorophenoxyacetic acid (2,4-D) and α-naphthalene acetic acid (NAA)] alone or in combination with cytokinin [6-benzylamino purine (BAP)] to induce callus. The cultures were subcultured for callus proliferation after every 4-week period. Callus induction frequency (explants with callus formation), fresh biomass, and texture of callus were noted after 4 weeks of subculture.

$$\text{Callus induction frequency (\%)} = \frac{\text{Number of explants producing callus}}{\text{Total number of explants inoculated}} \times 100$$

Preparation of extracts and GC-MS analysis. The methanolic extracts of each sample (bulb scales) and bulb scale calli (2, 4-D–induced, 0.5 mg/L) were prepared according to protocol of Hussain et al. (2019). The samples were shade-dried at room temperature

Table 1. Effect of different concentrations and combinations of plant growth regulators (PGRs) on callus induction from bulb scale explant in *C. asiaticum*.

PGRs	Concn (mg/L)	Callusing frequency (%)	Callus texture
Control	0	0 f	—
2,4-D	0.25	66.67 ± 4.17 bc	Compact
	0.50	95.83 ± 4.17 a	Compact
	0.75	87.5 ± 7.22 ab	Compact
	1.0	87.5 ± 0.00 ab	Compact
BAP+NAA	0.5 + 1.0	83.33 ± 4.17 ab	Friable
	0.5 + 0.75	54.17 ± 11.02 cd	Friable
	0.75 + 0.5	45.83 ± 8.33 d	Friable
	1.0 + 0.5	37.5 ± 7.22 e	Friable

Each value represents the mean ± standard error of three repeated experiments. Mean values followed by different letters in the same column are significantly different from each other according to Duncan's multiple range test at $P \leq 0.05$ level.
BAP = 6-benzylamino purine; NAA = α-naphthalene acetic acid.

Received for publication 20 Mar 2025. Accepted for publication 12 May 2025.
Published online 8 Jul 2025.
This research work is funded by the Department of Biotechnology (DBT/2020/JH/1336), New Delhi, India, and ongoing research funding program (ORF-2025-375), King Saud University, Riyadh, Saudi Arabia.
The original contributions presented in the study are included in the article, further inquiries can be directed to the corresponding author.
The authors declare no conflicts of interest.
The first author is thankful to the Department of Biotechnology (DBT) for financial support given as a Senior Research Fellowship. The authors are also grateful to the laboratory facilities provided by the Department of Botany, Jamia Hamdard, New Delhi. The authors acknowledge the ongoing research funding program (ORF-2025-375), King Saud University, Riyadh, Saudi Arabia.
A.M. is the corresponding author. E-mail: amujib@jamiahamdard.ac.in.

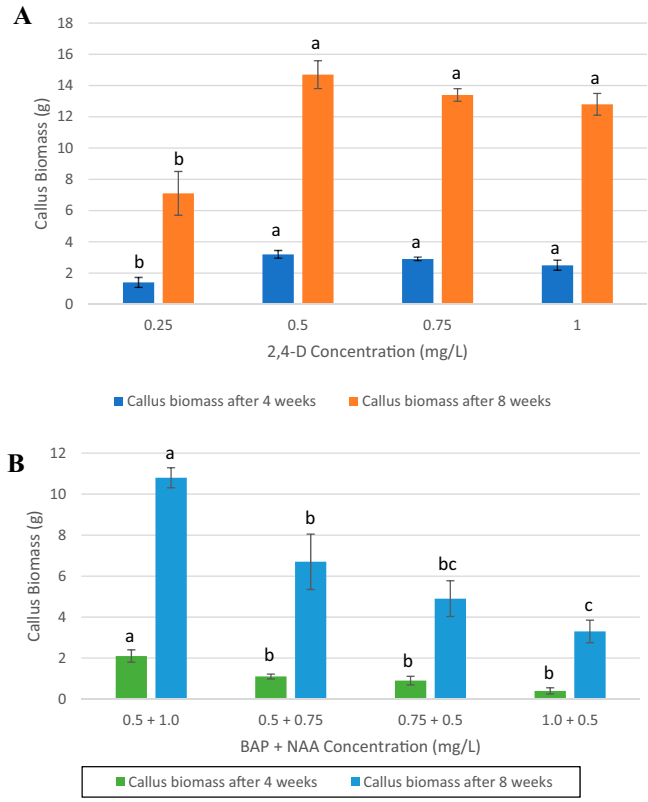

Fig. 2. Callus biomass growth (in grams) of *C. asiaticum* on (**A**) 2,4-D alone and (**B**) α-naphthalene acetic acid (NAA) + 6-benzylamino purine (BAP) (in combination) in amended Murashige and Skoog medium. Each value represents the mean ± standard error of three repeated experiments. Mean values followed by the different superscripts in a same column are significantly different from each other according to Duncan's multiple range test at $P \leq 0.05$ level.

and ground into fine powder using a mortar and pestle. Approximately 1.0 g of fine powder of each sample was extracted in methanol solvent (10 mL) in a rotary shaker at 120 rpm for 2 d. Then, the dissolved mixtures were filtered and subsequently concentrated under reduced pressure in a rotary evaporator. Thereafter, the extracts were redissolved in methanol and subjected to a GC-MS analysis. The metabolite profiling of methanolic extract of each sample was conducted using GC-MS-QP-2010 (Shimadzu, Tokyo, Japan) with the following program settings: instrument calibration was performed by adjusting the pressure and carrier gas flow rate; helium was a carrier gas with a column flow of 1.21 mL/min; and the injection temperature was 260 °C. The separation column used for GC-MS was the Rxi-5Sil MS GC Capillary Column (30 m, 0.25 mm inner diameter, 0.25 µm degrees of freedom). The oven temperature was programmed from 80 °C (hold time, 2 min) to 280 °C (hold time, 18 min). The ion source and interface temperatures were set at 220 °C and 270 °C, respectively, with a solvent cut time of 4.50 min. The total GC-MS running time was 35 min for each sample. The phytocompounds were identified by comparing their respective retention indices and mass spectra with those already listed in the National Institute of Standards and Technology (NIST) library and GCMS solution software (version 4.45 SP 1) (Shimadzu Corp., Columbia, MD, USA).

Antioxidant assays

Radical scavenging assay of DPPH. The DPPH radical scavenging assay was performed following the protocol of Baliyan et al. (2022). Briefly, 0.4 mL of methanolic extract was mixed with 3.6 mL of DPPH (0.024 w/v). An equivalent amount of methanol was used as blank/control and mixed with 3.6 ml DPPH. Then, the samples were kept at room temperature for 90 min in total dark, and each sample was prepared in triplicate. The absorbance of samples was finally measured at a wavelength of 517 nm using an ultraviolet Visible spectrophotometer (BL-295; Biolinkk, Delhi, India). The antioxidant activity was calculated using the following formula:

$$\text{Scavenging activity}\,\% = (A_C - A_S/A_C) \times 100$$

where A_C is the absorbance of the control and A_S is the absorbance of the sample.

Estimation of POD (EC 1.11.1.7) activity

Approximately 1.0 g of fresh samples (bulb scale and bulb scale callus) were finely homogenized with 10 mL of phosphate buffer (pH = approximately 7.0) and centrifuged at 12,000 rpm for 30 min at 4 °C. The supernatant was collected and used for the POD assay. The POD activity was checked using the methodology of Haida and Hakiman (2019), wherein the assay mixture contained 0.5 mL enzyme extracts, 1.0 mL of 10 mM potassium-phosphate buffer (pH = 7.0), 0.5 mL of 1% guaiacol solution, and 0.5 mL hydrogen peroxide solution (0.4%). The final volume was made by adding 2.5 mL of distilled water. Similarly, a standard group was also prepared, but it did not include the enzyme extract. Changes in the absorbance were measured at 470 nm for 30 min, and the enzymatic assay was calculated as A = ELC, where A is the absorbance, E is the extinction coefficient (6.39 $mM^{-1} \cdot cm^{-1}$), L is the path length (1.0 cm), and C is the enzyme concentration [units (U)/g fresh weight (FW) of samples].

Estimation of SOD (EC 1.15.1.1) activity

Fresh samples (1.0 g) were extracted with 10 mL of 0.5M phosphate buffer (pH = approximately 7.2) comprising 3 mM EDTA, 1.0% (w/v) PVP, and 0.2% (v/v) TritonX-100; finally, they were centrifuged at 12,000 rpm (4 °C) for 14 min. The supernatant was collected and subjected to the SOD assay. The reaction mixture (3 mL) contained 50 mM phosphate buffer (pH = approximately 7.8), 2.25 mM NBT solution, 3.0 mM EDTA, 10 µM riboflavin, 45 µM methionine, 1.0 M Na_2CO_3, and 10 µL of enzyme extract. As the control, a whole reaction mixture devoid of any enzyme extract was used. Thereafter, the mixture was incubated for 10 min at 25 °C under 15 W fluorescent lights, and the absorbance was measured at 560 nm against the control by using an ultraviolet VIS spectrophotometer. The amount of SOD required to cause a 50% reduction in NBT under test conditions was determined as one unit of SOD enzyme activity, and the enzymatic activity was expressed as U/mg FW.

Statistical analysis

All the in vitro culture experiments had a completely randomized design with six replicates per treatment, and every experiment was repeated thrice. The antioxidant assays were performed in triplicate, with each experiment repeated thrice. The resulting data were statistically analyzed by using an analysis of variance and SPSS software (version 25). Data were expressed as the mean ± standard error, and the significance of the mean differences was determined using Duncan's multiple range test at $P \leq 0.05$ (Duncan 1955) and the unpaired *t* test with SAS software (version 9.4; SAS Institute, Inc., Cary, NC, USA).

Results

Callus induction and proliferation

The influence of various PGRs such as 2,4-D (alone), NAA, and BAP (in combination) on induction of the callus from bulb scale explants was tested. The callus started to emerge from the basal portion of scales after 1 week of inoculation (Fig. 1A). The PGR-free MS served as a control in which no callus induction and growth were noted. The auxins 2,4-D and NAA are both crucial to

developing the callus; for example, 2,4-D alone showed a significantly higher incidence of callusing than that used in NAA and BAP combinations (Fig. 1B, Table 1). The callus induction frequency and FW were best noticed on 0.5 mg/L 2,4-D–fortified MS medium (95.83% and 3.2 g, respectively) (Fig. 2A). By further increasing the 2,4-D concentration, the callus induction efficiency was slightly reduced. In contrast, the lowest callusing (37.5%) was observed on MS medium with 1.0 mg/L BAP + 0.5 mg/L NAA added, with 0.4 g FW (Fig. 2B). After 8 weeks, a similar trend in callus biomass growth was noticed in all treatments. The explants treated with combinations of BAP and NAA produced a white friable callus, whereas those treated with 2,4-D alone produced a cream compact callus. All the other tested concentrations and combinations showed a mild to moderate callus formation response.

GC-MS analysis

The GC-MS analyses of methanolic extracts of bulb scales and bulb scales calli (8 weeks old, treated with 0.50 mg/L 2,4-D) of *C. asiaticum* revealed a total of 34 and 31 different phytocompounds, respectively (Table 2, Figs. 3 and 4). Among the bioactives exclusively identified in bulb scale extract were gamma-sitosterol ($C_{29}H_{50}O$), with the highest peak area of 7.64% and retention time (RT) of 27.425 min, followed by alpha-d-methylglucopyranoside ($C_7H_{14}O_6$; 5.55%), vitamin E ($C_{29}H_{50}O_2$; 3.26%), propylhexedrine ($C_{10}H_{21}N$; 2.33%), and 3′,5′-dimethoxyacetophenone ($C_{10}H_{12}O_3$; 2.09%), as well as other phytoconstituents such as cholestane-3-yl thiocyanate (0.71%), 1,3,4-eugenol (0.49%), and neophytadiene (0.41%). However, certain phytocompounds were detected in methanolic extract of bulb scale callus only, which include pyranone (3.18%), benzenepropanenitrile (3.18%), 24-ethylcholesterol (3.15%), and ethyl hexopyranoside (2.60%). Furthermore, approximately 19 bioactive compounds (41.3% of total compounds detected) were common in both samples at varied levels. The chemical structures of certain important phytocompounds (present in both extracts) have been presented in Fig. 5. The bulb scale extract had a higher

Table 2. Comparative list of phytocompounds detected using the gas chromatography-mass spectrometry technique for methanolic extracts of *C. asiaticum* samples.

No.	Compound	Retention time (min)		Peak area (%)		Molecular formula	Molecular wt
		In vivo bulb scale	Calli derived from bulb scale	In vivo bulb scale	Calli derived from bulb scale		
1	Pyranone	—	6.920	—	3.18	$C_6H_8O_4$	144
2	Benzenepropanenitrile	—	8.172	—	3.18	C_9H_9N	131
3	1,3,4-Eugenol	9.660	—	0.49	—	$C_{10}H_{12}O_2$	164
4	2-Cyclohexyl-3-isopropyl-pent-4-en-2-ol	10.034	—	0.97	—	$C_{14}H_{26}O$	210
5	Guanosine	11.065	11.069	4.24	34.61	$C_{10}H_{13}N_5O_5$	283
6	3′,5′-Dimethoxyacetophenone	12.106	—	2.09	—	$C_{10}H_{12}O_3$	180
7	alpha-d-methylglucopyranoside	13.165	—	5.55	—	$C_7H_{14}O_6$	194
8	Ethyl hexopyranoside	—	13.250	—	2.60	$C_8H_{16}O_6$	208
9	Methyl octadecanoate	13.552	13.549	0.27	0.87	$C_{19}H_{38}O_2$	298
10	Neophytadiene	14.690	—	0.41	—	$C_{20}H_{38}$	278
11	Palmitic acid, methyl ester	15.617	15.615	6.74	4.34	$C_{17}H_{34}O_2$	270
12	n-Octyl ether	16.012	16.010	1.24	0.65	$C_{16}H_{34}O$	242
13	Linoleic acid, methyl ester	17.231	17.229	7.74	5.56	$C_{19}H_{34}O_2$	294
14	Methyl elaidate	17.288	17.287	22.20	15.96	$C_{19}H_{36}O_2$	296
15	Stearic acid, methyl ester	17.523	17.521	5.71	3.82	$C_{19}H_{38}O_2$	298
16	4-Hydroxy-4-(6-methyl-3-cyclohexen-1-yl)-2-butanone	17.750	—	1.51	—	$C_{11}H_{18}O_2$	182
17	N-(3,5-dimethylphenyl)-N'-[2-(1-piperazinyl)ethyl]-Ethanedicarboxamide	—	17.783	—	1.50	$C_{16}H_{24}N_4O_2$	304
18	Octyl methoxycinnamate	17.970	17.963	0.51	0.44	$C_{18}H_{26}O_3$	290
19	Methyl 10-trans,12-cis-octadecadienoate	18.117	18.109	1.39	0.99	$C_{19}H_{34}O_2$	294
20	8,10-Heptacosanedione	18.477	—	0.31	—	$C_{27}H_{52}O_2$	408
21	Octanoic acid, 2-dimethylaminoethyl ester	18.917	—	0.63	—	$C_{12}H_{25}NO_2$	215
22	Carbonic acid, 2-dimethylaminoethyl neopentyl ester	—	18.921	—	0.39	$C_{10}H_{21}NO_3$	203
23	2-Monopalmitin	19.047	19.043	2.09	1.21	$C_{19}H_{38}O_4$	330
24	Arachidic acid methyl ester	19.285	19.282	0.93	0.80	$C_{21}H_{42}O_2$	326
25	2-Ethylhexyl (2E)-3-(4-methoxyphenyl)-2-propenoate	19.428	—	0.71	—	$C_{18}H_{26}O_3$	290
26	Oleyl amide	19.843	19.833	1.03	0.56	$C_{18}H_{35}NO$	281
27	Oleoyl chloride	—	20.155	—	0.73	$C_{18}H_{33}ClO$	300
28	12-Nitro-15-hexadecanolide	20.166	—	0.33	—	$C_{16}H_{29}NO_4$	299
29	Fumaric acid, 2-dimethylaminoethyl nonyl ester	—	20.382	—	1.23	$C_{17}H_{31}NO_4$	313
30	Propylhexedrine	20.421	—	2.33	—	$C_{10}H_{21}N$	155
31	Glycidyl oleate	20.545	20.540	5.39	3.62	$C_{21}H_{38}O_3$	338
32	alpha-Monostearin	20.737	20.737	1.35	0.66	$C_{21}H_{42}O_4$	358
33	Docosanoic acid, methyl ester	20.917	20.917	0.45	0.26	$C_{23}H_{46}O_2$	354
34	1,2-Benzenedicarboxylic acid	—	20.993	—	2.34	$C_{24}H_{38}O_4$	390
35	2,3-Dihydroxypropyl elaidate	22.333	22.334	4.09	2.83	$C_{21}H_{40}O_4$	356
36	Squalene	23.026	23.027	3.09	1.58	$C_{30}H_{50}$	410
37	Myristyl myristate	24.071	24.072	0.93	0.58	$C_{28}H_{56}O_2$	424
38	Stigmast-5-en-3-ol	—	25.225	—	0.58	$C_{29}H_{50}O$	414
39	Vitamin E	25.427	—	3.26	—	$C_{29}H_{50}O_2$	430
40	24-Epicampesterol	26.515	26.519	2.65	1.12	$C_{28}H_{48}O$	400
41	gamma-sitosterol	27.425	—	7.64	—	$C_{29}H_{50}O$	414
42	24-Ethylcholesterol	—	27.442	—	3.15	$C_{29}H_{50}O$	414
43	9,10-Dibromopentacosane	—	29.031	—	0.06	$C_{25}H_{50}Br_2$	508
44	Cholestan-3-yl thiocyanate	30.117	—	0.71	—	$C_{28}H_{47}NS$	429
45	(9z)-9-octadecenyl (9z)-9-hexadecenoate	32.166	—	1.05	—	$C_{34}H_{64}O_2$	504
46	Olealdehyde	—	32.172	—	0.62	$C_{18}H_{34}O$	266

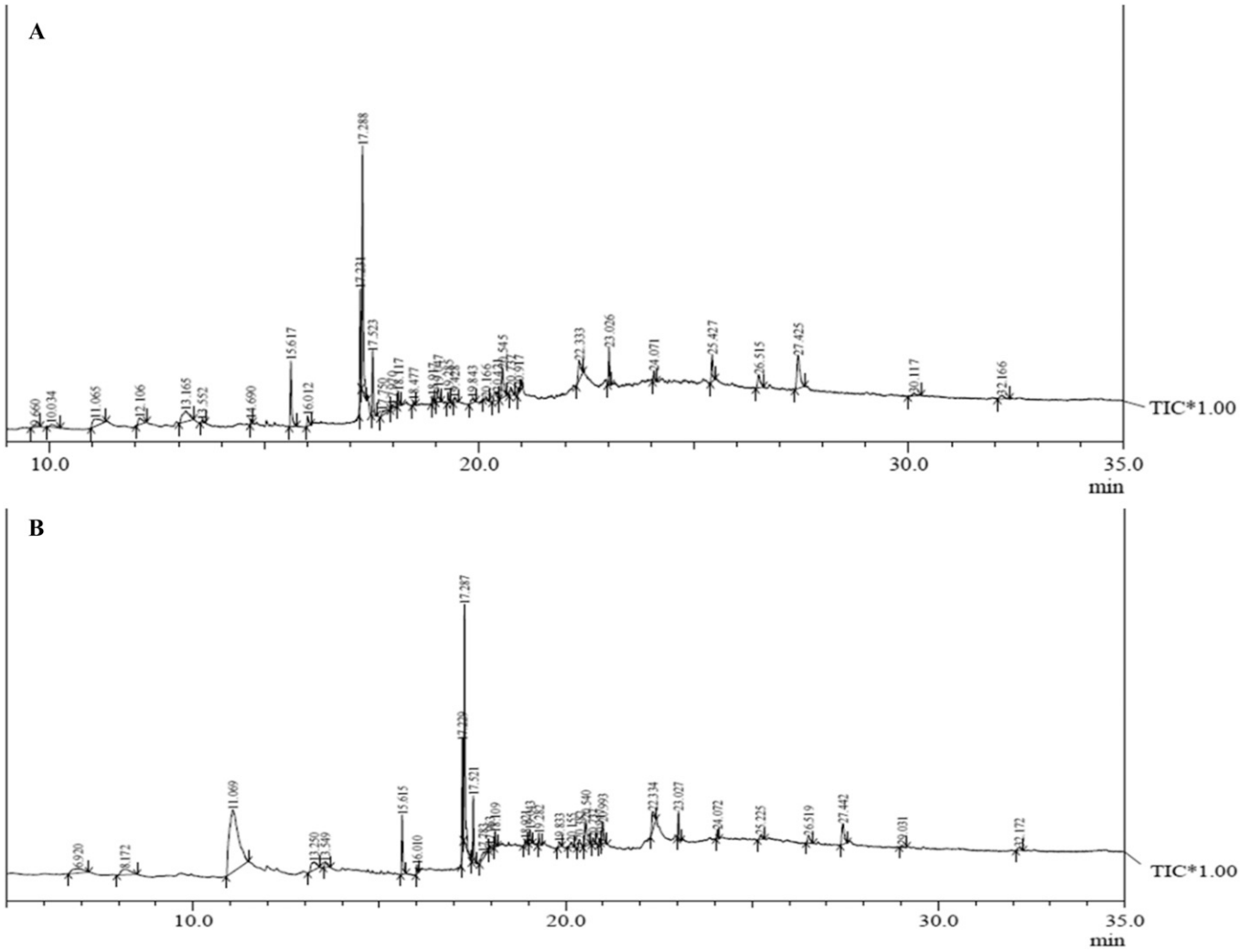

Fig. 3. Gas chromatography-mass spectrometry chromatograms of methanolic extracts of (**A**) bulb scale and (**B**) bulb scale callus of *C. asiaticum* representing the retention times with the corresponding peaks. The X-axis represents the time of elution of each compound and the Y-axis represents the intensity of the signal measured by the ion detector.

concentration of compounds when compared with callus extract. The contents of palmitic acid methyl ester (6.74%), linoleic acid (7.74%), and stearic acid (5.71%) were higher in bulb scale extract than in the callus tissue extract (4.34%, 5.56%, and 3.82%, respectively). Similarly, the amount of methyl elaidate was lower in callus extract (15.96%) than in the bulb scale sample (22.20%). Guanosine was one such compound with an almost eight-fold increase in callus extract (34.61%) as compared with bulb scale (4.24%). A similar difference was detected in the concentrations of squalene and 24-epicampesterol in bulb scale extract (3.09% and 2.65%, respectively) and in the callus sample (1.58% and 1.12%, respectively).

Antioxidant activities

The methanolic extracts of bulb scale and bulb scale callus of *C. asiaticum* were subjected to DPPH, POD, and SOD assays, and the results are summarized in Fig. 6. Overall, each antioxidant activity (DPPH, POD, and SOD) was slightly higher in callus tissue than in the bulb scale extract. For the DPPH assay, the callus extract exhibited higher scavenging activity (49.32%) than that of bulb scale extract (35.23%). Similarly, the highest POD activity was noticed in the callus sample (0.51 ± 0.01 U/g FW) compared with that in bulb scale (0.26 ± 0.02 U/g FW). A similar trend was also observed in SOD activity, whereby the callus extract showed a slight increment in SOD activity (1.06 ± 0.01 U/mg FW) as compared with the bulb scale extract, with SOD activity of 0.91 ± 0.02 U/mg FW.

Discussion

In this present study, a various responses in callus induction and callus morphology/texture were noted with different combinations and concentrations of PGRs. The function of PGRs in stimulating callus is important because these signaling elements control cell cycle enzymes, and exogenous PGR application alters other endogenous hormone levels, which causes plant cell wall dissipation and the development process (Qahtan et al. 2022). In our study, prolific callus induction was noted from bulb scale on MS medium supplied with 2, 4-D as compared with NAA and BAP combinations because the chemical structures of PGRs differ, and each has a distinct impact on metabolic responses (Al-Hamidi et al. 2023). Similarly, 2,4-D showed high efficacy for inducing callus in several investigated plants such as *Rhodophiala pratensis* (Trujillo-Chacón et al. 2020) and *Saussurea costus* (Khan et al. 2021), and these observations were in accordance with our findings. Additionally, 2,4-D at a lower concentration promotes callogenesis because its higher concentration may act as a herbicide, leading to browning and reduced viability of tissues.

One of the most popular techniques for producing a consistent and continuous supply of secondary metabolites is in vitro propagation (Espinosa-Leal et al. 2018). To identify and compare metabolic profiles of the mother plant and the callus tissue of *C. asiaticum* obtained in vitro, the GC-MS analysis was conducted. The analyses revealed a total of 19 phytocompounds present in both the samples, but they differed in their contents; however, some phytocompounds were exclusively present in two different samples. Callus extract

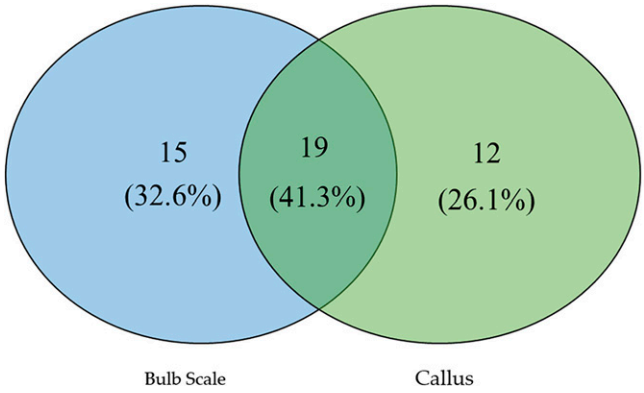

Fig. 4. Venn diagram representing the proportion of phytocompounds detected by gas chromatography-mass spectrometry in bulb scale and callus extracts of *C. asiaticum*.

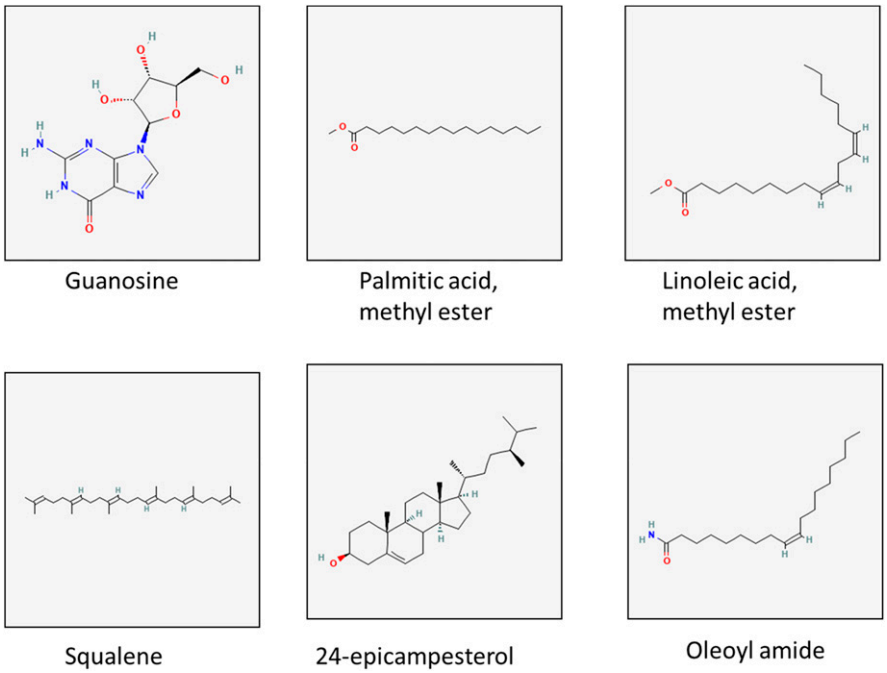

Fig. 5. Chemical structure of some important phytocompounds identified in both the extracts (in vivo and callus samples). Images were taken from the PubChem compound database, National Centre for Biotechnology Information.

showed the exclusive presence of phytocompounds like pyranone, benzenepropane nitrile, oleoyl chloride, and stigmast-5-en-3-ol. This differential presence of bioactives in each sample occurred because of their spatial and temporal regulation; in other words, secondary metabolites accumulate in specific cells, organs, and tissues at specific growth phases/conditions (Pérez-Mejía et al. 2024). Other factors like PGR exposure, number of subcultures, genotype, photoperiod, and humidity also play crucial roles in determining the metabolic profile of each sample. Thus, an in vitro callus culture can be considered a potent source when producing therapeutically significant phytocompounds for commercial purposes.

The bulb scale extract displayed the presence of a wide variety of compounds with high pharmacological values. One such compound is gamma-sitosterol, which is widely known to exhibit antidiabetic, anti-inflammatory, antioxidant, anticancerous, and antihyperlipidemic activities (Ambavade et al. 2014). Vitamin E has a role in cancer prevention and protecting against neurodegenerative diseases because of its antioxidant and anti-inflammatory effects (Szymańska et al. 2017). Eugenol demonstrated a broad spectrum of biological activity (i.e., antifungal, antibacterial, anti-inflammatory, anticancer, antioxidant, analgesic, and antiparasitic properties) (Abdou et al. 2021). Similarly, the callus-derived methanolic extract showed the presence of various phytocompounds such as stigmast-5-en-3-ol, 24-ethylcholesterol and olealdehyde. Stigmast-5-en-3-ol belongs to the phytosterol category and has antidiabetic, antiproliferative, and antioxidative effects (Bolar et al. 2016; Fernando et al. 2018; Sujatha et al. 2010). Zhang et al. (2021) reported various activities of cholesterol and its derivatives against diseases and found antimicrobial, anticancerous, antipsychotic, and anti-inflammatory properties. Several other important phytocompounds such as guanosine, methyl ester of palmitic acid, linoleic acid, stearic acid, arachidic acid, squalene, and 24-epicampesterol were detected in both the extracts with diverse pharmacological activities. Squalene is a triterpenoid with anti-inflammatory, antineoplastic, and antiatherosclerotic effects (Lou-Bonafonte et al. 2018). Linoleic acid acts as a protective agent against various health disorders like diabetes, cancer, obesity, and atherosclerosis (Yang et al. 2015). Pyranone and its derivatives have applications in leukemia treatment (Peroković et al. 2020). Benzenepropane nitrile is a volatile compound that prevents various cardiovascular and neurodegenerative disorders (Lasekan and Azeez 2014).

The cultivated cells and regenerated tissues frequently experience stress under in vitro systems, leading to the production of ROS that

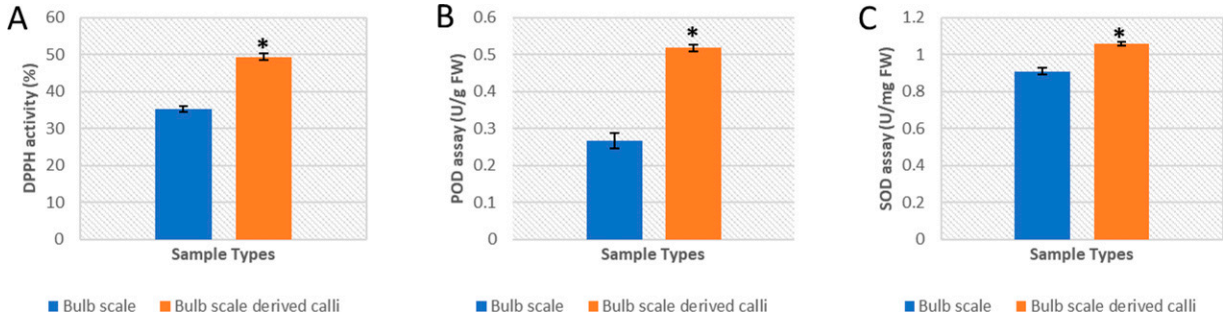

Fig. 6. Antioxidant activities (**A**) 2, 2-diphenyl-1-picrylhydrazyl (DPPH) activity, (**B**) peroxidase (POD) activity, and (**C**) superoxide dismutase (SOD) activity of bulb scale and bulb scale callus of *C. asiaticum*. Each value represents the mean ± standard error of three replicates. *Significant at $P \leq 0.05$ according to Student's unpaired *t* test.

lower the cell survival rate (Malik et al. 2018). To combat ROS toxicity, plant cells have inherent enzymatic (such as SOD, POD, CAT, glutathione reductase, and ascorbate peroxidase) and nonenzymatic defensive mechanisms. In our study, the antioxidant activities (DPPH, POD, and SOD) of callus were high compared with those of bulb scale extract, thus revealing adverse cellular conditions during cultivation. Similar reports of increased antioxidant activity in the in vitro samples of other investigated plant species are available (Abdulhafiz et al. 2020; Bansal et al. 2024b; Mishra et al. 2021).

Conclusions

The present study described the phytocompounds' profiles of bulb scale and bulb scale callus in *C. asiaticum*. The bulb scales of *C. asiaticum* produced a positive response when inducing callus when exposed to different PGR concentrations. The obtained calli were subject to metabolite profiling using the GC-MS technique. Callus derived in vitro revealed the presence of diverse phytocompounds in varied quantities, indicating a rich reservoir of medicinally important metabolites like terpenoids, sterols, fatty acids. Because GC-MS allows the separation of low-molecular-weight and volatile compounds, other chromatographic techniques like ultra-high-performance liquid chromatography coupled with mass spectrometry or liquid chromatography tandem mass spectrometry should also be used. Additionally, the antioxidant activities (DPPH, POD, and SOD) of tissues were higher in the in vitro samples as compared with the in vivo samples. Thus, the present investigation may contribute to in silico molecular docking and bioprospecting studies of advanced pharmacological applications such as drug discovery.

References Cited

Abdou A, Elmakssoudi A, Amrani AE, JamalEddine J, Dakir M. 2021. Recent advances in chemical reactivity and biological activities of eugenol derivatives. Med Chem Res. 30(5): 1011–1030. https://doi.org/10.1007/s00044-021-02712-x.

Abdulhafiz F, Mohammed A, Kayat F, Zakaria S, Hamzah Z, Pamuru RR, Gundala PB, Reduan MFH. 2020. Micropropagation of *Alocasia longiloba* Miq and comparative antioxidant properties of ethanolic extracts of the field-grown plant, in vitro propagated and in vitro-derived callus. Plants. 9(7):816. https://doi.org/10.3390/plants9070816.

Al-Hamidi AO, Al-Hadedy SH, Bashi AZ. 2023. Effect of 2, 4-D and NAA in callus induction and differentiation from different explants of *Moringa oleifera* Lam. IOP Conf Ser: Earth Environ Sci. 1252(1):012091. https://doi.org/10.1088/1755-1315/1252/1/012091.

Ambavade SD, Misar AV, Ambavade PD. 2014. Pharmacological, nutritional, and analytical aspects of β-sitosterol: A review. Orient Pharm Exp Med. 14(3):193–211. https://doi.org/10.1007/s13596-014-0151-9.

Ashwini N, Rajanna L. 2022. GC-MS Analysis of the in vitro leaf derived callus extracts of *Ichnocarpus frutescens* (L)W.T.Aiton. Int J Life Sci Pharm Res. https://doi.org/10.22376/ijpbs/lpr.2022.12.3.L58-65.

Bakrim S, Benkhaira N, Bourais I, Benali T, Lee L-H, Omari NE, Sheikh RA, Goh KW, Ming LC, Bouyahya A. 2022. Health benefits and pharmacological properties of stigmasterol. Antioxidants. 11(10):1912. https://doi.org/10.3390/antiox11101912.

Baliyan S, Mukherjee R, Priyadarshini A, Vibhuti A, Gupta A, Pandey RP, Chang C-M. 2022. Determination of antioxidants by DPPH radical scavenging activity and quantitative phytochemical analysis of Ficus religiosa. Molecules. 27(4): 1326. https://doi.org/10.3390/molecules27041326.

Bansal M, Mujib A, Bansal Y, Dewir YH, Mendler-Drienyovszki N. 2024a. An efficient in vitro shoot organogenesis and comparative GC-MS metabolite profiling of *Gaillardia pulchella* Foug. Horticulturae. 10(7):728. https://doi.org/10.3390/horticulturae10070728.

Bansal Y, Mujib A, Mamgain J, Dewir YH, Rihan HZ. 2023. Phytochemical composition and detection of novel bioactives in anther callus of *Catharanthus roseus* L. Plants. 12(11):2186. https://doi.org/10.3390/plants12112186.

Bansal Y, Mujib A, Mamgain J, Syeed R, Mohsin M, Nafees A, Dewir YH, Mendler-Drienyovszki N. 2024b. Integrated GC-MS and UPLC-ESI-QTOF-MS based untargeted metabolomics analysis of in vitro raised tissues of *Digitalis purpurea* L. Front Plant Sci. 15:1433634. https://doi.org/10.3389/fpls.2024.1433634.

Benjamin ED, Ishaku GA, Peingurta FA, Afolabi AS. 2019. Callus culture for the production of therapeutic compounds. Am J Plant Biol. 4(4):76. https://doi.org/10.11648/j.ajpb.20190404.14.

Bibi A, Khan MA, Adil M, Mashwani ZU. 2018. Production of callus biomass and antioxidant secondary metabolites in black cumin. JAPS: J Animal Plant Sci. 28(5).

Bolar B, George J, Meshram GA. 2016. Isolation and biological evaluation of (24r) stigmast-5-en-3-ol from *Cassia fistula* bark. World J Pharm Res. 6(1):696–704.

Cardoso JC, de Oliveira MEBS, De Ci Cardoso F. 2019. Advances and challenges on the *in vitro* production of secondary metabolites from medicinal plants. Hortic Bras. 37(2):124–132. https://doi.org/10.1590/s0102-053620190201.

Danquah CA, Minkah PAB, Agana TA, Moyo P, Ofori M, Doe P, Rali S, Osei Duah Junior I, Amankwah KB, Somuah SO, Nugbemado IN, Maharaj VJ, Bhakta S, Gibbons S. 2022. The phytochemistry and pharmacology of tulbaghia, allium, crinum and cyrtanthus: 'Talented' taxa from the Amaryllidaceae. Molecules. 27(14): 4475. https://doi.org/10.3390/molecules27144475.

Duncan DB. 1955. Multiple range and multiple F tests. Biometrics. 11(1):1. https://doi.org/10.2307/3001478.

Efferth T. 2019. Biotechnology applications of plant callus cultures. Engineering. 5(1):50–59. https://doi.org/10.1016/j.eng.2018.11.006.

Espinosa-Leal CA, Puente-Garza CA, García-Lara S. 2018. *In vitro* plant tissue culture: Means for production of biological active compounds. Planta. 248(1):1–18. https://doi.org/10.1007/s00425-018-2910-1.

Fatima T, Mujib A, Bansal Y, Dewir YH, Mendler-Drienyovszki N. 2024. Indirect organogenesis of *Calendula officinalis* L. and comparative phytochemical studies of field-grown and *in vitro*-regenerated tissues. Agronomy. 14(8):1743. https://doi.org/10.3390/agronomy14081743.

Fernando IPS, Sanjeewa KKA, Ann YS, Ko CI, Lee SH, Lee WW, Jeon YJ. 2018. Apoptotic and antiproliferative effects of stigmast-5-en-3-ol from *Dendronephthya gigantea* on human leukemia HL-60 and human breast cancer MCF-7 cells. Toxicol In Vitro. 52:297–305. https://doi.org/10.1016/j.tiv.2018.07.007.

Georgiev V, Ivanov I, Pavlov A. 2020. Recent progress in Amaryllidaceae biotechnology. Molecules. 25(20):4670. https://doi.org/10.3390/molecules25204670.

Haida Z, Hakiman MA. 2019. Comprehensive review on the determination of enzymatic assay and nonenzymatic antioxidant activities. Food Sci Nutr. 7(5):1555–1563. https://doi.org/10.1002/fsn3.1012.

Hazrati R, Zare N, Asghari-Zakaria R, Sheikhzadeh P, Johari-Ahar M. 2022. Factors affecting the growth, antioxidant potential, and secondary metabolites production in hazel callus cultures. AMB Express. 12(1):109. https://doi.org/10.1186/s13568-022-01449-z.

Hussain SA, Ahmad N, Anis M, Alatar AA. 2019. Influence of meta-topolin on in vitro organogenesis in *Tecoma stans* L., assessment of genetic fidelity and phytochemical profiling of wild and regenerated plants. Plant Cell Tiss Organ Cult. 138(2):339–351. https://doi.org/10.1007/s11240-019-01631-5.

Ka S, Merindol N, Sow AA, Singh A, Landelouci K, Plourde MB, Pépin G, Masi M, Di Lecce R, Evidente A, Seck M, Berthoux L, Chatel-Chaix L, Desgagné-Penix I. 2021. Amaryllidaceae alkaloid cherylline inhibits the replication of dengue and zika viruses. Antimicrob Agents Chemother. 65(9). 10.1128/aac.00398-21.

Khan A, Shah AH, Ali N. 2021. In-vitro propagation and phytochemical profiling of a highly medicinal and endemic plant species of the Himalayan region (*Saussurea costus*). Sci Rep. 11(1):23575. https://doi.org/10.1038/s41598-021-03032-1.

Lasekan O, Azeez S. 2014. Chemo-preventive activities of common vegetables' volatile organic compounds (VOCs). Pharm Anal Acta. 5:2.

Lou-Bonafonte JM, Martínez-Beamonte R, Sanclemente T, Surra JC, Herrera-Marcos LV, Sanchez-Marco J, Arnal C, Osada J. 2018. Current insights into the biological action of squalene. Mol Nutr Food Res. 62(15):e1800136. https://doi.org/10.1002/mnfr.201800136.

Luo P, Feng X, Liu S, Jiang Y. 2024. Traditional uses, phytochemistry, pharmacology and toxicology of *Ruta graveolens* L.: A critical review and future perspectives. Drug Des Devel Ther. 18:6459–6485. https://doi.org/10.2147/DDDT.S494417.

Mahomoodally MF, Sadeer NB, Suroowan S, Jugreet S, Lobine D, Rengasamy KRR. 2021. Ethnomedicinal, phytochemistry, toxicity and pharmacological benefits of poison bulb–*Crinum asiaticum* L. South Afr Bot. 136:16–29. https://doi.org/10.1016/j.sajb.2020.06.004.

Malik M, Wachol M, Pawlowska B. 2018. Liquid culture systems affect morphological and biochemical parameters during *Rosa canina* plantlets *in vitro* production. Not. Bot. Horti Agrobot. Cluj-Napoca. 46:58–64.

Mishra MK, Pandey S, Niranjan A, Misra P. 2021. Comparative analysis of phenolic compounds from wild and *in vitro* propagated plant *Thalictrum foliolosum* and antioxidant activity of various crude extracts. Chem Pap. 75(9):4873–4885. https://doi.org/10.1007/s11696-021-01708-6.

Murashige T, Skoog F. 1962. A revised medium for rapid growth and bio assays with tobacco tissue cultures. Physiol. Plant. 15(3):473–497. https://doi.org/10.1111/j.1399-3054.1962.tb08052.x.

Murthy HN, Joseph KS, Paek KY, Park SY. 2023. Bioreactor systems for micropropagation of plants: present scenario and future prospects.

Front Plant Sci. 14:1159588. https://doi.org/10.3389/fpls.2023.1159588.
Ozden M, Karaaslan M. 2011. Effects of cytokinin on callus proliferation associated with physiological and biochemical changes in *Vitis vinifera* L. Acta Physiol Plant. 33(4):1451–1459. https://doi.org/10.1007/s11738-010-0681-9.
Pérez-Mejía N, Villarreal ML, Sánchez-Carranza JN, González-Maya L, González-Cortazar M, Ortíz-Caltempa A, Alvarez L. 2024. Phytochemical profiles and cytotoxic activity of *Bursera fagaroides* (Kunth) Engl. leaves and its callus culture. Plants. 13(12):1622. https://doi.org/10.3390/plants13121622.
Peroković VP, Car Ž, Usenik A, Opačak-Bernardi T, Jurić A, Tomić S. 2020. Adamantyl pyran-4-one derivatives and their in vitro antiproliferative activity. Mol Divers. 24(1):253–263. https://doi.org/10.1007/s11030-019-09948-1.
Priyadharshini S, Manokari M, Shekhawat MS. 2020. *In vitro* conservation strategies for the critically endangered Malabar river lily (*Crinum malabaricum* Lekhak & Yadav) using somatic embryogenesis and synthetic seed production. South Afr Bot. 135:172–180. https://doi.org/10.1016/j.sajb.2020.08.030.
Qahtan AA, Faisal M, Alatar AA, Abdel-Salam EM. 2022. Callus-mediated high-frequency plant regeneration, phytochemical profiling, antioxidant activity and genetic stability in *Ruta chalepensis* L. Plants. 11(12):1614. https://doi.org/10.3390/plants11121614.
Rahman MA, Sharmin R, Uddin MN, Rana MS, Ahmed NU. 2012. Antibacterial, antioxidant and cytotoxic properties of *Crinum asiaticum* bulb extract. Bangla J Microbiol. 28(1):1–5. https://doi.org/10.3329/bjm.v28i1.11801.
Rakhi SA, Hara Y, Islam MS, Manome T, Alam S, Emon NU, Al-Mansur MA, Kuddus MR, Sarkar MR, Ishibashi M, Ahmed F. 2024. Isolation of bioactive phytochemicals from *Crinum asiaticum* L. along with their cytotoxic and TRAIL-resistance abrogating prospect assessment. Heliyon. 10(3):e25049. https://doi.org/10.1016/j.heliyon.2024.e25049.
Sanyal R, M M, Pandey S, Nandi S, Biswas P, Dewanjee S, Gopalakrishnan AV, Jha NK, Jha SK, Joshee N, Pandey DK, Dey A, Shekhawat MS. 2023. Biotechnological interventions and production of galanthamine in *Crinum* spp. Appl Microbiol Biotechnol. 107(7–8):2155–2167. https://doi.org/10.1007/s00253-023-12444-0.
Sujatha S, Anand S, Sangeetha KN, Shilpa K, Lakshmi J, Balakrishnan A, Lakshmi BS. 2010. Biological evaluation of (3β)-stigmast-5-en-3-ol as potent anti-diabetic agent in regulating glucose transport using invitro model. Int J Diabetes Mellitus. 2(2):101–109. https://doi.org/10.1016/j.ijdm.2009.12.013.
Sura S, Solleti VSK. 2020. Assessment of anti urolithiatic potentials of *Crinum asiaticum* bulbs by *in vitro* and in vivo approaches. JYP. 12(2s):s76–s81. https://doi.org/10.5530/jyp.2020.12s.51.
Syeed R, Mujib A, Bansal Y, Mohsin M, Nafees A, Malik MQ, Mamgain J, Ejaz B, Dewir YH, Magyar-Tábori K. 2024. Tissue-specific natural synthesis of galanthamine in *Zephyranthes* species and its accumulation in different *in vitro*-grown organs following methyl jasmonate treatment. Plants. 13(14):1931. https://doi.org/10.3390/plants13141931.
Szymańska R, Nowicka B, Kruk J. 2017. Vitamin E—occurrence, biosynthesis by plants and functions in human nutrition. Mini Rev Med Chem. 17(12):1039–1052. https://doi.org/10.2174/1389557516666160725094819.
Tan WN, Shahbudin FN, Kamal N, Tong WY, Leong CR, Lim JW. 2019. Volatile constituents of the leaf essential oil of *Crinum asiaticum* and their antimicrobial and cytotoxic activities. J Essential Oil Bearing Plants. 22(4):947–954. https://doi.org/10.1080/0972060X.2019.1683079.
Trujillo-Chacón LM, Pastene-Navarrete ER, Bustamante L, Baeza M, Alarcón-Enos JE, Cespedes-Acuña CL. 2020. In vitro micropropagation and alkaloids analysis by GC–MS of Chilean Amaryllidaceae plants: *Rhodophialapratensis*. Phytochem Anal. 31(1):46–56. https://doi.org/10.1002/pca.2865.
Wang Y, Zhai W, Cheng S, Li J, Zhang H, 11. 2023. Surface-functionalized design of blood-contacting biomaterials for preventing coagulation and promoting hemostasis. Friction. 11(8):1371–1394. https://doi.org/10.1007/s40544-022-0710-x.
Wan H, Zhou S, Li C, Zhou H, Wan H, Yang J, Yu L. 2024. Ant colony algorithm-enabled back propagation neural network and response surface methodology based ultrasonic optimization of safflower seed alkaloid extraction and antioxidant. Ind Crop Prod. 220:119191. https://doi.org/10.1016/j.indcrop.2024.119191.
Yang B, Chen H, Stanton C, Ross RP, Zhang H, Chen YQ, Chen W. 2015. Review of the roles of conjugated linoleic acid in health and disease. J Funct Foods. 15:314–325. https://doi.org/10.1016/j.jff.2015.03.050.
Zhang K, Li T, Shan X, Lu R, Zhang S, Xu H. 2021. Cholesterol: Bioactivities, structural modification, mechanisms of action, and structure-activity relationships. Mini Rev Med Chem. 21(14):1830–1848. https://doi.org/10.2174/1389557521666210105123320.